Geophysical Research Letters

RESEARCH LETTER
10.1029/2020GL092194

Key Points:

- Smoke from the extraordinary 2020 Californian wild fires traveled within 3–4 days toward Europe
- Highest Aerosol Optical Thickness ever measured in the free troposphere over Leipzig, Germany, Central Europe, with ground-based lidar
- Unique opportunity for a first assessment of the aerosol optical profiles of the spaceborne wind lidar mission Aeolus

Correspondence to:
H. Baars,
baars@tropos.de

Citation:
Baars, H., Radenz, M., Floutsi, A. A., Engelmann, R., Althausen, D., Heese, B., et al. (2021). Californian wildfire smoke over Europe: A first example of the aerosol observing capabilities of Aeolus compared to ground-based lidar. *Geophysical Research Letters*, *48*, e2020GL092194. https://doi.org/10.1029/2020GL092194

Received 18 DEC 2020
Accepted 7 MAR 2021

Californian Wildfire Smoke Over Europe: A First Example of the Aerosol Observing Capabilities of Aeolus Compared to Ground-Based Lidar

Holger Baars[1], Martin Radenz[1], Athena Augusta Floutsi[1], Ronny Engelmann[1], Dietrich Althausen[1], Birgit Heese[1], Albert Ansmann[1], Thomas Flament[2], Alain Dabas[2], Dimitri Trapon[2], Oliver Reitebuch[3], Sebastian Bley[4], and Ulla Wandinger[1]

[1]Leibniz Institute for Tropospheric Research (TROPOS), Leipzig, Germany, [2]CNRM, Université de Toulouse, Météo-France, CNRS, Toulouse, France, [3]DLR, Institute of Atmospheric Physics, Oberpfaffenhofen, Germany, [4]European Space Agency (ESA) ESRIN, Frascati, Italy

Abstract In September 2020, extremely strong wildfires in the western United States of America (i.e., mainly in California) produced large amounts of smoke, which was lifted into the free troposphere. These biomass-burning-aerosol (BBA) layers were transported from the US west coast toward central Europe within 3–4 days turning the sky milky and receiving high media attention. The present study characterizes this pronounced smoke plume above Leipzig, Germany, using a ground-based multiwavelength-Raman-polarization lidar and the aerosol/cloud product of ESA's wind lidar mission Aeolus. An exceptional high smoke-AOT >0.4 was measured, yielding to a mean mass concentration of 8 μg m^{-3}. The 355 nm lidar ratio was moderate at around 40–50 sr. The Aeolus-derived backscatter, extinction and lidar ratio profiles agree well with the observations of the ground-based lidar PollyXT considering the fact that Aeolus' aerosol and cloud products are still preliminary and subject to ongoing algorithm improvements.

Plain Language Summary In September 2020, extremely strong wildfires in the western USA (i.e., mainly in California) produced large amounts of smoke. These biomass burning aerosol (BBA) layers were transported from the US west coast towards central Europe within 3-4 days. This smoke plume was observed above Leipzig, Germany, for several days turning the sky milky and receiving high media attention - it was the highest perturbation of the troposphere in terms of AOT ever observed over Leipzig. The first smoke plume arrived on 11 September 2020, just in time for a regular overpass of the Aeolus satellite of the European Space Agency (ESA). Aeolus accommodates the first instrument in space that actively measures profiles of a horizontal wind component in the troposphere and lower stratosphere. Aeolus has been launched to improve weather forecasts while assimilating the Aeolus wind profile data in near–real time. But Aeolus also delivers profiles of aerosol and cloud optical properties as spin-off products. We performed a first assessment of the aerosol profiling capabilities of Aeolus while precisely analyzing the smoke plume above Leipzig with a ground-based multiwavelength-Raman-polarization lidar. But we also show the dramatic impact of fires in the western USA on atmospheric conditions over central Europe.

1. Introduction

On August 22, 2018, the European Space Agency (ESA) successfully launched the Earth Explorer Mission Aeolus (Stoffelen et al., 2005). The scope of this mission is to measure profiles of one horizontal wind component (mainly the west-east direction) in the troposphere and stratosphere (European Space Agency, 2008; Reitebuch et al., 2020; Stoffelen et al., 2005; Straume et al., 2020) and to improve weather forecasts while assimilating the Aeolus wind profile data in near–real time (Horányi et al., 2015a, 2015b; Rennie & Isaksen, 2020). On-board of this satellite is the Atmospheric Laser Doppler Instrument (ALADIN), which is a high spectral resolution (HSR, Lux et al., 2020; Wandinger, 1998) Doppler lidar (LIght Detection And Ranging). ALADIN is the first lidar instrument on a European satellite and the first instrument in space that actively can measure profiles of an horizontal wind component (Baars, Herzog, et al., 2020; Martin et al., 2021; Reitebuch, 2012; Witschas et al., 2020). It follows the very successful CALIPSO mission (Winker et al., 2009) with its elastic polarization lidar CALIOP on-board, which is delivering aerosol and cloud

profiles since 2006 (e.g., Young et al., 2018). While the main focus of the Aeolus mission is to obtain atmospheric horizontal winds, the lidar is also capable to retrieve aerosol and cloud optical properties as spin-off products (Ansmann et al., 2007; Flamant et al., 2008) via the HSR lidar (HSRL) technique. This technique is a spaceborne novelty. Thus, one of the goals of this Earth Explorer Mission is to prove the concept of this new technology in space.

While the exploitation of the aerosol products and algorithm development of Aeolus is still ongoing, we want to present a first glimpse on the Aeolus' capabilities to measure vertical aerosol profiles. For this purpose, we investigated dense smoke layers observed near Leipzig, Germany, originating from very strong and intense wildfires in the western United States (US) of America. In 2020, wildfires, for example in California, have been dramatically intensive, also triggering the discussion of an increased risk of wildfires due to climate change (Brando et al., 2019; Wehner et al., 2017). The resulting smoke plumes from such fires, once lifted to the free troposphere and/or lower stratosphere (UTLS) can travel several thousand kilometers and influence the aerosol load even in very remote regions (Baars et al, 2011, 2012; Fromm et al., 2010; Kloss et al., 2019). In late summer 2017, an intense event of smoke-plume advection from Canadian wildfires was monitored in central Europe (Ansmann et al., 2018; Haarig et al., 2018; Hu et al., 2019; Khaykin et al., 2018). At that time, tropospheric smoke plumes were remarkable but stratospheric smoke was even more intense, lasting for more than half a year above the tropopause over the European continent (Baars et al., 2019). Similar observations were made in the Southern Hemisphere during the recent Australian fires (austral summer 2019/2020, Ohneiser et al., 2020; Khaykin et al., 2020).

Here, we present an example of the most recent smoke event originating from fires in south-western North America (mainly in California) and observed over Leipzig, Germany in the frame of the German initiative for the Experimental Validation and Assimilation of Aeolus observations (EVAA, e.g., Baars, Geiβ, et al., 2020; Geiβ et al., 2019). The observations were performed on September 11, 2020 at the Leibniz Institute of Tropospheric Research (TROPOS) in Leipzig. Our objective is to present a first assessment on the Aeolus aerosol observing capabilities and to show the dramatic impact of fires in the western United States of America on atmospheric conditions over central Europe—it was the highest perturbation of the troposphere in terms of Aerosol Optical Thickness (AOT) ever observed at TROPOS since the start of the regular lidar observations in 1997. Aeolus is currently the only spaceborne lidar able to measure independently backscatter and extinction of aerosol and clouds and thus deliver the particle-type-depending extinction-to-backscatter ratio, called lidar ratio. It therefore provides valuable information on the radiative properties of these smoke aerosols. Furthermore, Aeolus is the only satellite in space that measures simultaneously aerosol properties together with profiles of the horizontal wind speed. This unique configuration is expected to improve the predictions of such extreme events as well as air quality forecasts (European Space Agency, 2008; Horányi et al., 2015a; Letertre-Danczak et al., 2020).

2. Californian Smoke Over Central Europe

Figure 1 shows the atmospheric conditions over Leipzig, Germany on September 11, 2020 as measured with the ground-based multiwavelength-Raman-polarization lidar PollyXT (Engelmann et al., 2016) organized within the voluntary, scientific network PollyNET (Baars et al., 2016) and part of EARLINET/ACTRIS (Pappalardo et al., 2014). The time-height plot of the uncalibrated attenuated backscatter coefficient at 1064 nm is presented to indicate the backscatter intensity of atmospheric particles. While blueish colors represent no significant particle concentration and thus almost pure molecular scattering, green and reddish colors indicate a moderate to high aerosol load. White colors represent very strong backscattering caused by clouds. Besides some low-level clouds and local aerosol below 2.5 km before 05:00 UTC, first aerosol layers, namely smoke from Californian fires, arrived at an altitude of about 12 km at 03:00 UTC as seen in Figure 1. The arrival at this height range is most probably a result of the higher wind speeds in the jet stream region. Later through the day, smoke layers were observed throughout the whole troposphere down to about 4.5 km altitude and thus well above the local planetary boundary layer (PBL). The total AOT in Leipzig increased to values of 0.6 at 380 nm and 0.4 at 532 nm between 14:00 and 17:00 UTC as observed with an AERONET sun photometer (Giles et al., 2019) on this day. Smoke layers from this event could be observed at TROPOS until 14 September.

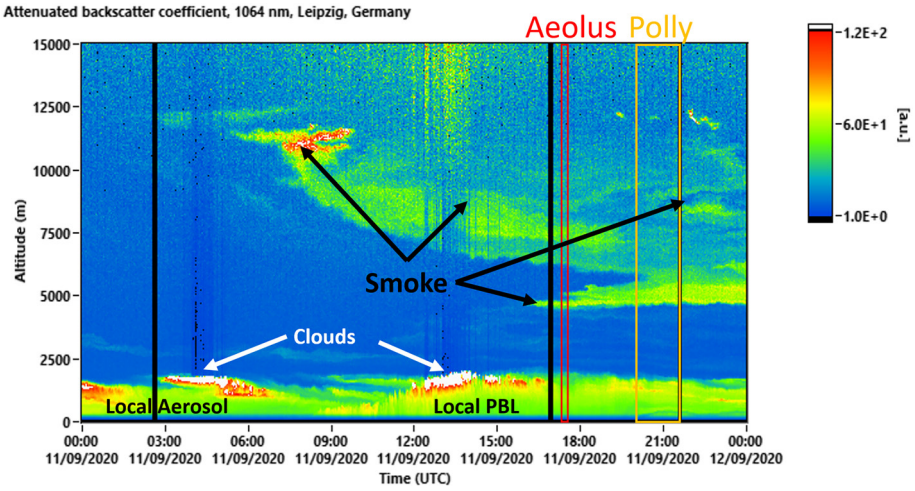

Figure 1. Time-height plot of the uncalibrated attenuated backscatter coefficient at 1064 nm measured at ground in Leipzig, Germany, with the multiwavelength-Raman polarization lidar PollyXT. The time of the overpass is indicated as red rectangle while the data analysis period of the ground-based lidar data is highlighted in orange. No data is available during regular depolarization calibrations (black).

To characterize the atmospheric state over Leipzig on September 11, 2020, we exemplary analyze the air-masses arriving at noon (12 UTC) at about 8.5 km—the height of the estimated center of the smoke layer according to Figure 1. A 10-day FLEXPART (Pisso et al., 2019; Stohl et al., 2002) backward simulation of 500 air parcels originating at Leipzig between 8.3 and 8.7 km height on September 11, 2020 at 12 UTC was performed. Five clusters were generated by grouping the simulated air parcels based on their location at three-hourly intervals. The result is shown in Figure 2. Cluster size is indicated by the size of the dots, with larger clusters representing more air parcels. Colors are assigned to clusters that are closest to each other

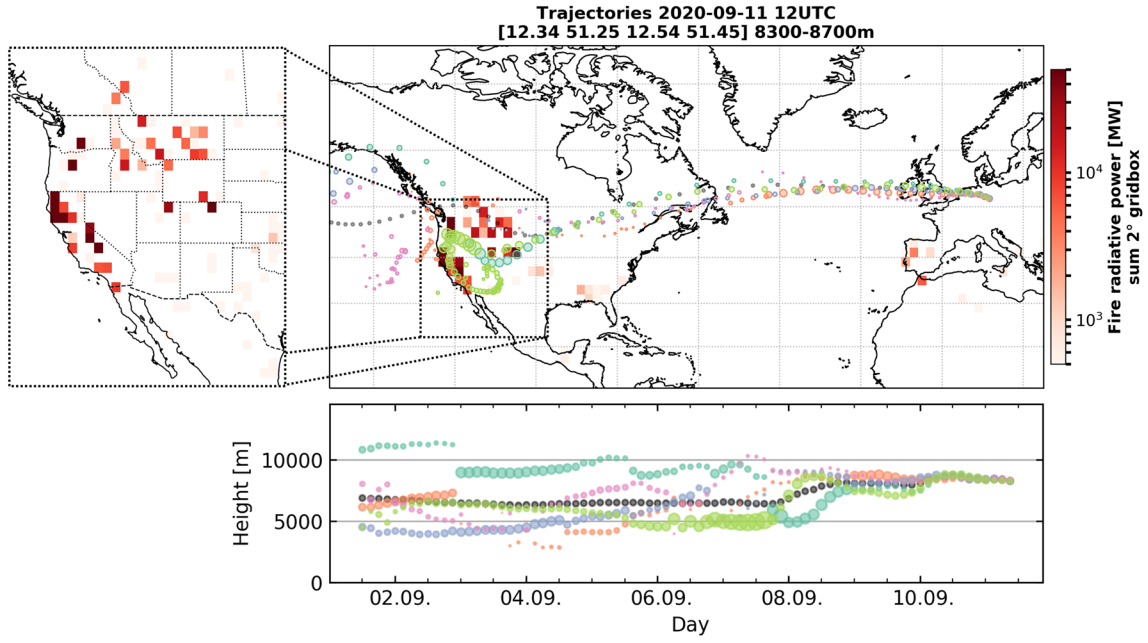

Figure 2. Airmass origin at Leipzig on September 11, 2020 underlaid with MODIS derived fire radiative power: Clusters of air parcel positions ending at Leipzig between 8.3 and 8.7 km height at 12 UTC (see text for further description). Geographic location (top panel) and heights (bottom panel) of the clusters (indicated by color) are shown. Dot size denotes the size of each cluster. Dark gray dots denote the mean position of all particles. MODIS derived fire radiative power was gridded to 2°. Only fire detections between 31 August and September 7, 2020 are included. A zoomed map of the fire radiative power gridded to 1° in the western US is shown at the left.

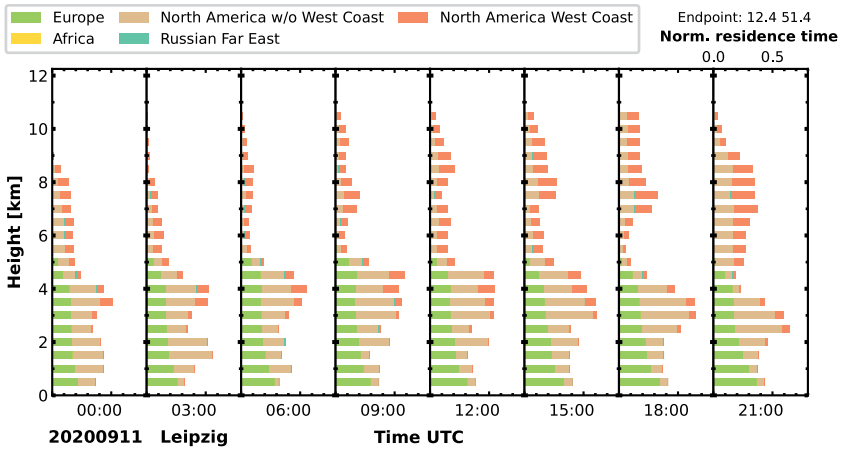

Figure 3. Airmass source estimate on the September 11, 2020 for airmasses arriving at Leipzig, Germany. The estimate is based on 10-day backward simulations using a reception height of 5 km.

at two consecutive times. However, they do not represent a continuous trajectory, as the particles for each cluster might have changed.

This backward simulation proves that the airmasses arriving over Leipzig at 8.5 km height at 12:00 UTC originated from the west coast of North America, where intense fires were taking place during this time as indicated by the very high fire radiative power as shown in Figure 2, left (Giglio, 2016). Fire frequency and strength in California increased during the first week of September. Slightly weaker fires were observed in Oregon, Washington and Montana. Due to the prevailing winds, the travel time of the smoke from the US West Coast to Europe was only 3–4 days. The airmass was transported across the Atlantic Ocean in a long filament at approximately 51°N on 1 day only (9 September).

The time-height cross-section of airmass source (Figure 3, Radenz et al., 2021) generalizes the findings from the single time and height analysis as shown in Figure 2. Air parcel positions are calculated every 3 h and for height intervals of 500 m. At each step, the residence time is summed up for each region, whenever particles were below the reception height during the backward simulation. The reception height of 5 km was set to agree to with typical injection heights caused by wildfires of similar strength (Val Martin et al., 2018) and shall not be confused with arrival height of the plume at Leipzig. The grouped residence time profiles are then visualized in the time-height-cross-section. According to Figure 3, airmasses originating at the west coast of North America were present over Leipzig during the whole day, being especially prominent above 4 km after 9 UTC. The results suggest that in this case, smoke injection into the middle troposphere was sufficient to be subject to long-range transport. Please note, that the actual injection could also occur at lower altitudes, but would still be covered by the 5 km threshold. As shown in Figure 2, the lifting to 8.5 km occurred during the transport on the 8 September.

It can therefore be concluded that the strong wildfires in California in 2020 produced large amounts of smoke, which were then transported toward Europe.

3. Aerosol Optical Profiles of Aeolus Compared to Ground-Based Lidar

Aeolus reached central Europe around 16:45 UTC on September 11, 2020, as shown in Figure 4. Here, the backscatter coefficient of Aeolus retrieved with the HSRL technique (called Standard Correction Algorithm [SCA] product; Flamant et al., 2017; Huber et al., 2016) is visualized with VirES (Santillan et al., 2019) for this overpass. Despite the noise in the backscatter product, this intense aerosol plume is clearly visible ranging from Leipzig to southern Norway (greenish colors). The very strong backscatter values (bright yellow) over central Norway were caused by clouds also indicated by deep blue colors below (no signal due to complete attenuation of laser beam in optically thick clouds). Note that Aeolus aerosol profiles are currently only available with a horizontal resolution of 87 km and vertical resolution from 500 to 2000 m depending on altitude (500–1000 m in the troposphere).

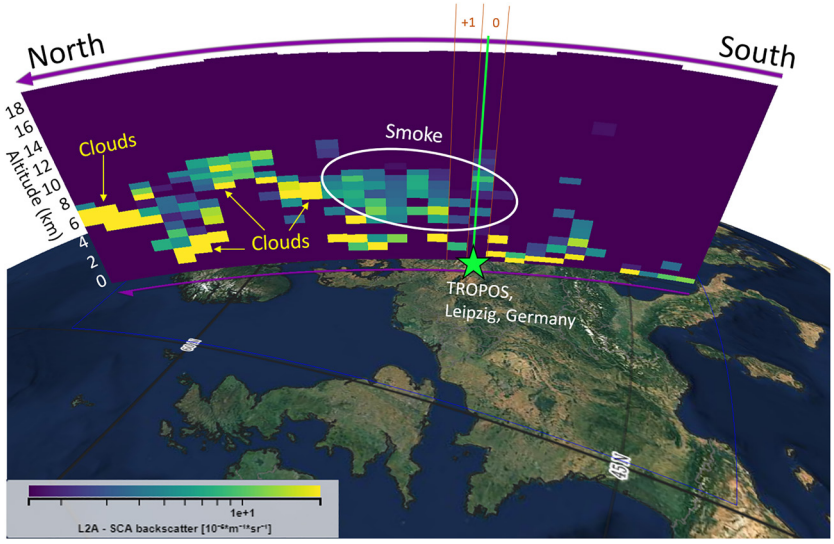

Figure 4. Aeolus particle backscatter coefficient profiles at 355 nm as derived with the standard correction algorithm (SCA) during the overpass on September 11, 2020 at around 16:45 UTC as visualized with VirES. Colors represent the backscatter coefficient value from 1.5 to 20 Mm^{-1} sr^{-1} plotted on a logarithmic scale. The location of the ground based measurements at Leipzig, Germany, is indicated by the green star. The green vertical line represents the laser beam of the ground-based lidar.

We used the ground-based Raman lidar observations made 2–3 h later at Leipzig to compare them with the Aeolus observations made around 100 km north-west of Leipzig (indicated with "+1" in Figure 4) instead of presenting the comparison with the closest overpass. Due to the strong solar background at the time of the overpass (around 17:45 local solar time), Raman retrievals (Ansmann et al., 1992) of the ground-based lidar delivering the backscatter and extinction coefficient independently were not possible. Backward trajectories indicate that airmasses traveled around 3 h from the Aeolus track 100 km north toward Leipzig. For this reason, we used the night time observation made between 20:00 and 21:30 UTC for the comparison as visualized in Figure 1. Considering no significant changes in the aerosol distribution within the smoke plume over this short time and thus only advection as result of the mean wind fields, a good collocation criterion is found to allow the comparison of the ground-based Raman retrievals with the HSRL retrievals of Aeolus. A similar procedure (Papagiannopoulos et al., 2016; Tesche et al., 2013) has also been applied for Calibration/Validation activities of the spaceborne lidar on-board CALIPSO (Winker et al., 2009).

Figure 5 shows the comparison of the ground-based Raman-polarization lidar PollyXT with the Aeolus observation as described. The particle backscatter and extinction coefficient, along with the corresponding lidar ratio (extinction-to-backscatter ratio), are shown (Raman methodology for PollyXT and HSR methodology for Aeolus). For Aeolus, the HSR product SCA and a HSR product obtained by smoothing two vertical bins called "SCA mid bin" are presented. These two products are standard output.

As the Aeolus lidar data are very noisy and the provided uncertainties are currently overestimated, the quality flags included in the Aeolus aerosol spin-off (L2A) product are not yet mature (Reitebuch et al., 2020). For this reason, we applied the following quality control criteria for Aeolus data:

1. Exclude negative backscatter and extinction coefficient values
2. Absolute value of the provided extinction error must be less than 100 and 275 Mm^{-1} for SCA and SCA mid bin, respectively

As seen in Figure 5, left, an excellent agreement regarding the backscatter coefficient (at 355 nm) between the ground-based lidar (black thick line) and the Aeolus SCA algorithms (red and blue lines) is found for the lofted smoke layer between 4 and 12 km. In the PBL, Aeolus obtains higher values than the lidar at Leipzig, probably due to the coarse horizontal resolution of Aeolus and the spatio-temporal variations in terms of optical particles properties within the PBL (e.g., due to hygroscopic growth). In addition, sporadic contamination of the 87 km aggregated Aeolus observation with small boundary layer clouds cannot be ruled out.

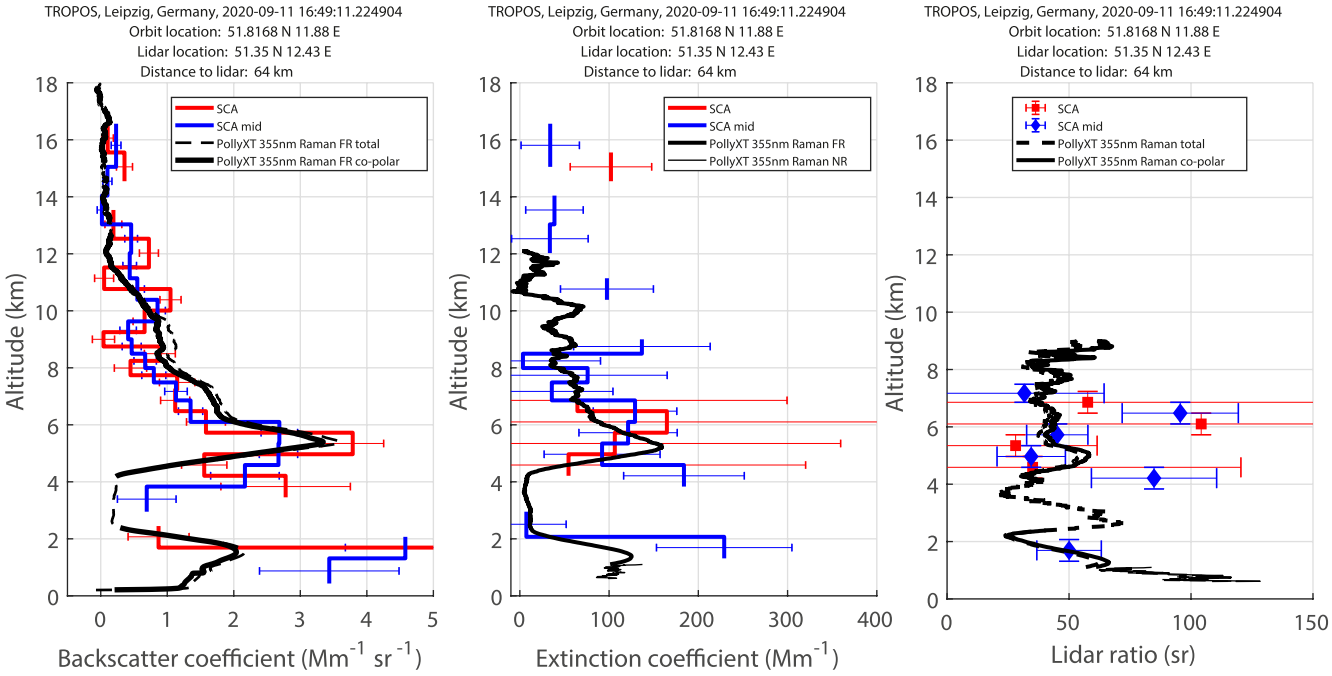

Figure 5. Comparison of the optical profiles provided by Aeolus (red and blue) and the ground-based EARLINET lidar PollyXT (black lines). The particle backscatter coefficient (left), the particle extinction coefficient (center), and the corresponding lidar (extinction-to-backscatter) ratio is shown. The ground-based backscatter observations (dashed line) are converted to Aeolus-like, that means, co-polar, profiles (solid line) for comparability. The mean coordinates and distance of the 87 km long Aeolus observations to the ground-based lidar are given as well.

It should be noted that since Aeolus is only able to detect the co-polar backscatter component of the circularly polarized emitted light (Ansmann et al., 2007; Flamant et al., 2008), the ground-based PollyXT observations at 355 nm (dotted, black line) had to be transformed to an Aeolus-like profile by means of the measured particle linear depolarization ratio - for more details see, for example, Baars, Geiβ, et al. (2020). Nevertheless, as the smoke particles arriving from the US did almost not depolarize the light during the backscattering process (particle linear depolarization ratio at 355 nm below 10% according to PollyXT), almost no difference between the total particle backscatter profile and the Aeolus-like (co-polar) backscatter profile is evident.

The extinction coefficient profiles of Aeolus are in reasonable agreement with the ground-based ones (Figure 5, center panel). Due to the utilization of molecular scattering processes for the extinction retrievals, the profiles are naturally much noisier compared to the backscatter ones. Nevertheless, both shape and magnitude of the extinction profile agree well within the pronounced smoke layer between 4 and 8 km for both retrievals. The SCA mid-bin algorithm provides more robust results due to averaging of two neighboring height bins and should be prioritized for extinction analyses. Sporadic values for extinction above 8.5 km are provided by both algorithms, an effect that is attributed to instrumental noise. Compared to the ground-based lidar profiles, these values above 8.5 km are unrealistically high. A series of algorithm improvements (including quality flags, improved calibration and error estimates etc.) are still under development and are foreseen to avoid such artifacts in future. Therefore, the current Aeolus aerosol optical data is still flagged as preliminary.

The message for this example case is that Aeolus is able to measure - as a first spaceborne lidar - backscatter and extinction independently in pronounced aerosol layers, and thus is able to directly derive the lidar ratio as shown in Figure 5, right. We thus focus in the following on the intensive aerosol properties within the main smoke layer below 8 km. Within this pronounced aerosol layer, the agreement between the lidar ratio observed by the ground-based lidar (and converted to the co-polar (Aeolus-like) component) and the one observed by Aeolus is reasonable (please remind, that current Aeolus uncertainties are overestimated and thus unrealistically high). The PollyXT observations yield a lidar ratio of the smoke of about 40–50 sr at 355 nm, which is in excellent agreement with former observations of long-range transported smoke (Haarig

et al., 2018; Ohneiser et al., 2020). Aeolus measured values within the same range, even though some outliers in the smoke region exist (at around 6 km). These outliers are mainly caused by the noisy signals but algorithm development to reduce these effects are ongoing. As for the extinction, the SCA mid bin algorithm is to be preferred against the SCA for the lidar ratio analysis.

The missing depolarization component of Aeolus did not restrict the characterization of the dominant aerosol types in the lofted smoke layer, since the particles were mainly spherical and thus non-depolarizing. However, in cases of a more heterogeneous aerosol field, polarization capabilities would have been highly desirable also with respect to a potential aerosol type identification (e.g., polarizing mineral dust and volcanic ash) and aerosol/cloud discrimination (Ansmann et al., 2011; Baars et al., 2017; Pappalardo et al., 2013). Such capabilities are implemented in the future EarthCARE mission (Wandinger et al., 2016).

From the multiwavelength Raman polarization PollyXT measurements, it is also possible to derive the smoke mass concentration as described by Mamouri and Ansmann (2016) and Ansmann et al. (2020). For this purpose, an extinction-to-volume conversion factor of 0.169×10^{-12} Mm at 532 nm and a particle density of 1.3 g cm^{-3} have been used for the smoke layer. These values, which are required for the conversion of particle extinction coefficient to mass concentration, correspond to semi-aged smoke according to Ansmann et al. (2020). The procedure yields to a maximum smoke mass concentration of 22 $\mu g\ m^{-3}$ in the smoke layer peak around 5 km (maximum extinction coefficient of 160 and 100 Mm^{-1} at 355 and 532 nm, respectively). Integrating the mass concentration over the entire smoke layer leads to a total mass of 64,757 $\mu g\ m^{-2}$ that has been observed at Leipzig between 20:00 UTC and 21:30 UTC (corresponding to a mean concentration of 8 $\mu g\ m^{-3}$). The AOT of the smoke layer (from 3.8 to 11 km) was 0.45 and 0.29 at 355 and 532 nm, respectively, and thus about 2/3 of the total AOT, showing the dramatic impact of the Californian wildfires on the Central European troposphere.

4. Conclusions

The potential of Aeolus to independently retrieve aerosol backscatter and extinction coefficients was demonstrated in this study by means of a comparison to a high-quality ground based lidar. An extreme event of smoke advection from the US west coast which was observed over Leipzig, Germany, Central Europe, served as an example. Besides Aeolus' observing capabilities, this study demonstrated that strong wildfires, such as the ones occurred in western US in 2020, can emit huge smoke amounts, which are comparable to volcanic eruptions (Peterson et al., 2018). These extraordinary smoke plumes are able to travel relatively fast over large distances between the continents and thus might influence radiation, clouds, and weather at even remote places usually not directly affected by wildfires and several thousand kilometers away from the source.

The intense smoke plume, which arrived at the measurement location of Leipzig on September 11, 2020, caused a perturbation of the troposphere for 4–5 days. A smoke-related AOT of 0.45 at 355 nm was measured above Leipzig with estimated maximum and mean mass concentrations of the smoke of 22 and 8 $\mu g\ m^{-3}$, respectively. Aeolus captured this smoke plume near the ground-based station of Leipzig on the first day of the event during its regular overpass. Despite the coarse horizontal (≈ 87 km) and vertical (500–1000 m) resolution of Aeolus' aerosol optical profiles, it was shown that the HSRL technique can be successfully applied from space. Within the main smoke layer, the Aeolus-derived backscatter, extinction and lidar ratio profiles compare well with the high-quality ground based lidar considering the still ongoing algorithm improvements and uncertainty estimation refinements.

Measuring the lidar ratio directly from space is a spaceborne novelty and boosts aerosol-cloud interaction research into a new era. The results presented here indicate that Aeolus is partly capable of filling the gap between the ending CALIPSO and the upcoming EarthCARE mission (Illingworth et al., 2015). However, further sensitivity studies on how well Aeolus is able to correctly determine extinction and backscatter coefficients in less pronounced aerosol layers are still ongoing and one main focus of current Cal/Val activities.

Data Availability Statement

The ground-based Polly lidar data is visualized at polly.tropos.de and will become publicly available via the data portal of the European Aerosols, Clouds and Trace gases Research Infrastructure (ACTRIS) when its implementation phase is completed. Aeolus aerosol spin-off data used in this publication is not yet publicly available, but, after reprocessing in spring 2021, including improved radiometric calibration and quality flags, an updated data set will become freely available via ESA services (i.e., https://aeolus-ds.eo.esa.int/oads/access/ and the online VirES tool at https://aeolus.services/). Nevertheless, to allow the FAIR data principles, all data used for this study are available at zenodo.org under https://doi.org/10.5281/zenodo.1115995.

Acknowledgments
This research has been supported by the German Federal Ministry for Economic Affairs and Energy (BMWi) under grant no. 50EE1721C. Authors also acknowledge support through ACTRIS-2 under grant agreement no. 654109 from the European Union's Horizon 2020 research and innovation program, and through PoLiCyTa from the German Federal Ministry of Education and Research (BMBF) under grant no. 01LK1603A. We also appreciate very much the fruitful discussions within the EVAA consortium (LMU, DWD, DLR), with the "Aeolus DISC" team, and the Aeolus Team of ESA. The processor development, improvement and product re-processing preparation are performed by the Aeolus DISC (Data, Innovation and Science Cluster), which involves DLR, DoRIT, ECMWF, KNMI, CNRS, S&T, ABB, and Serco, in close cooperation with the Aeolus PDGS (Payload Data Ground Segment). The analysis has been performed in the framework of the Aeolus Scientific Calibration & Validation Team (ACVT).

References

Ansmann, A., Baars, H., Chudnovsky, A., Mattis, I., Veselovskii, I., Haarig, M., et al. (2018). Extreme levels of Canadian wildfire smoke in the stratosphere over central Europe on 21–22 August 2017. *Atmospheric Chemistry and Physics*, *18*(16), 11831–11845. https://doi.org/10.5194/acp-18-11831-2018

Ansmann, A., Ohneiser, K., Mamouri, R.-E., Knopf, D. A., Veselovskii, I., Baars, H., et al. (2020). Tropospheric and stratospheric wildfire smoke profiling with lidar: Mass, surface area, CCN and INP retrieval. *Atmospheric Chemistry and Physics Discussions*, *2020*, 1–45. https://doi.org/10.5194/acp-2020-1093

Ansmann, A., Petzold, A., Kandler, K., Tegen, I., Wendisch, M., Müller, D., et al. (2011). Saharan mineral dust experiments SAMUM-1 and SAMUM-2: What have we learned? *Tellus B: Chemical and Physical Meteorology*, *63*(4), 403. https://doi.org/10.1111/j.1600-0889.2011.00555.x

Ansmann, A., Wandinger, U., Le Rille, O., Lajas, D., & Straume, A. G. (2007). Particle backscatter and extinction profiling with the space-borne high-spectral-resolution Doppler lidar ALADIN: Methodology and simulations. *Applied Optics*, *46*(26), 6606–6622. https://doi.org/10.1364/AO.46.006606

Ansmann, A., Wandinger, U., Riebesell, M., Weitkamp, C., & Michaelis, W. (1992). Independent measurement of extinction and backscatter profiles in cirrus clouds by using a combined Raman elastic-backscatter lidar. *Applied Optics*, *31*, 7113–7131. https://doi.org/10.1364/AO.31.007113

Baars, H., Ansmann, A., Althausen, D., Engelmann, R., Artaxo, P., Pauliquevis, T., et al. (2011). Further evidence for significant smoke transport from Africa to Amazonia. *Geophysical Research Letters*, *38*(20). https://doi.org/10.1029/2011gl049200

Baars, H., Ansmann, A., Althausen, D., Engelmann, R., Heese, B., Müller, D., et al. (2012). Aerosol profiling with lidar in the Amazon Basin during the wet and dry season. *Journal of Geophysical Research: Atmospheres*, *117*(D21). https://doi.org/10.1029/2012jd018338

Baars, H., Ansmann, A., Ohneiser, K., Haarig, M., Engelmann, R., Althausen, D., et al. (2019). The unprecedented 2017–2018 stratospheric smoke event: Decay phase and aerosol properties observed with the EARLINET. *Atmospheric Chemistry and Physics*, *19*(23), 15183–15198. https://doi.org/10.5194/acp-19-15183-2019

Baars, H., Geiß, A., Wandinger, U., Herzog, A., Engelmann, R., Bühl, J., et al. (2020a). First results from the German Cal/Val activities for Aeolus. *EPJ Web of Conferences*, *237*, 01008. https://doi.org/10.1051/epjconf/202023701008

Baars, H., Herzog, A., Heese, B., Ohneiser, K., Hanbuch, K., Hofer, J., et al. (2020b). Validation of Aeolus wind products above the Atlantic Ocean. *Atmospheric Measurement Techniques*, *13*(11), 6007–6024. https://doi.org/10.5194/amt-13-6007-2020

Baars, H., Kanitz, T., Engelmann, R., Althausen, D., Heese, B., Komppula, M., et al. (2016). An overview of the first decade of PollyNET: An emerging network of automated Raman-polarization lidars for continuous aerosol profiling. *Atmospheric Chemistry and Physics*, *16*(8), 5111–5137. https://doi.org/10.5194/acp-16-5111-2016

Baars, H., Seifert, P., Engelmann, R., & Wandinger, U. (2017). Target categorization of aerosol and clouds by continuous multiwavelength-polarization lidar measurements. *Atmospheric Measurement Techniques*, *10*(9), 3175–3201. https://doi.org/10.5194/amt-10-3175-2017

Brando, P. M., Paolucci, L., Ummenhofer, C. C., Ordway, E. M., Hartmann, H., Cattau, M. E., et al. (2019). Droughts, wildfires, and forest carbon cycling: A pantropical synthesis. *Annual Review of Earth and Planetary Sciences*, *47*(1), 555–581. https://doi.org/10.1146/annurev-earth-082517-010235

Engelmann, R., Kanitz, T., Baars, H., Heese, B., Althausen, D., Skupin, A., et al. (2016). The automated multiwavelength Raman polarization and water-vapor lidar PollyXT: The neXT generation. *Atmospheric Measurement Techniques*, *9*(4), 1767–1784. https://doi.org/10.5194/amt-9-1767-2016

European Space Agency. (2008). *ADM-Aeolus Science Report – SP-1311*. European Space Agency (ESA). Retrieved from https://earth.esa.int/documents/10174/1590943/AEOL002.pdf

Flamant, P., Cuesta, J., Denneulin, M.-L., Dabas, A., & Huber, D. (2008). ADM-Aeolus retrieval algorithms for aerosol and cloud products. *Tellus A: Dynamic Meteorology and Oceanography*, *60*(2), 273–286. https://doi.org/10.1111/j.1600-0870.2007.00287.x

Flamant, P. H., Lever, V., Martinet, P., Flament, T., Cuesta, J., Dabas, A., et al. (2017). *ADM-Aeolus L2A algorithm theoretical baseline document, particle spin-off products*. Retrieved from https://earth.esa.int/eogateway/documents/20142/37627/Aeolus-L2A-ATBD.pdf

Fromm, M., Lindsey, D. T., Servranckx, R., Yue, G., Trickl, T., Sica, R., et al. (2010). The untold story of pyrocumulonimbus. *Bulletin of the American Meteorological Society*, *91*(9), 1193–1210. https://doi.org/10.1175/2010bams3004.1

Geiß, A., Lehmann, V., Leinweber, R., Reitebuch, O., & Weissmann, M. (2019). Methodology and case studies for the validation of aeolus observations by means of radar wind profilers. In *ESA living planet symposium 2019, Milan, Italy*. Retrieved from https://lps19.esa.int/NikalWebsitePortal/living-planet-symposium-2019/lps19/Agenda/AgendaItemDetail?id=64570099-bea7-4b8f-a54b-5b6ad81fa342

Giglio, L. (2016). *MODIS Aqua and Terra 1 km Thermal Anomalies and Fire Locations V006 NRT. NASA Land Atmosphere Near real-time Capability for EOS Fire Information for Resource Management System*. https://doi.org/10.5067/FIRMS/MODIS/MCD14DL.NRT.006

Giles, D. M., Sinyuk, A., Sorokin, M. G., Schafer, J. S., Smirnov, A., Slutsker, I., et al. (2019). Advancements in the Aerosol Robotic Network (AERONET) Version 3 database - automated near-real-time quality control algorithm with improved cloud screening for Sun photometer aerosol optical depth (AOD) measurements. *Atmospheric Measurement Techniques*, *12*(1), 169–209. https://doi.org/10.5194/amt-12-169-2019

Haarig, M., Ansmann, A., Baars, H., Jimenez, C., Veselovskii, I., Engelmann, R., et al. (2018). Depolarization and lidar ratios at 355, 532, and 1064 nm and microphysical properties of aged tropospheric and stratospheric Canadian wildfire smoke. *Atmospheric Chemistry and Physics*, *18*(16), 11847–11861. https://doi.org/10.5194/acp-18-11847-2018

Horányi, A., Cardinali, C., Rennie, M., & Isaksen, L. (2015a). The assimilation of horizontal line-of-sight wind information into the ECMWF data assimilation and forecasting system. Part I: The assessment of wind impact. *Quarterly Journal of the Royal Meteorological Society*, *141*(689), 1223–1232. https://doi.org/10.1002/qj.2430

Horányi, A., Cardinali, C., Rennie, M., & Isaksen, L. (2015b). The assimilation of horizontal line-of-sight wind information into the ECMWF data assimilation and forecasting system. Part II: The impact of degraded wind observations. *Quarterly Journal of the Royal Meteorological Society*, *141*(689), 1233–1243. https://doi.org/10.1002/qj.2551

Hu, Q., Goloub, P., Veselovskii, I., Bravo-Aranda, J.-A., Popovici, I. E., Podvin, T., et al. (2019). Long-range-transported Canadian smoke plumes in the lower stratosphere over northern France. *Atmospheric Chemistry and Physics*, *19*(2), 1173–1193. https://doi.org/10.5194/acp-19-1173-2019

Huber, D., Dabas, A., & Lever, V. (2016). *Aeolus level 2a processor input/output data definition*. Retrieved from https://earth.esa.int/eogateway/documents/20142/37627/Aeolus-L2A-IODD-ATBD-SRN.zip

Illingworth, A. J., Barker, H. W., Beljaars, A., Ceccaldi, M., Chepfer, H., Clerbaux, N., et al. (2015). The EarthCARE satellite: The next step forward in global measurements of clouds, aerosols, precipitation, and radiation. *Bulletin of the American Meteorological Society*, *96*, 1311–1332. https://doi.org/10.1175/BAMS-D-12-00227.1

Khaykin, S., Legras, B., Bucci, S., Sellitto, P., Isaksen, L., Tence, F., et al. (2020). The 2019/20 Australian wildfires generated a persistent smoke-charged vortex rising up to 35 km altitude. *Communications Earth & Environment*, *1*(1), 1–12. https://doi.org/10.1038/s43247-020-00022-5

Khaykin, S. M., Godin-Beekmann, S., Hauchecorne, A., Pelon, J., Ravetta, F., & Keckhut, P. (2018). Stratospheric smoke with unprecedentedly high backscatter observed by Lidars above Southern France. *Geophysical Research Letters*, *45*(3), 1639–1646. https://doi.org/10.1002/2017gl076763

Kloss, C., Berthet, G., Sellitto, P., Ploeger, F., Bucci, S., Khaykin, S., et al. (2019). Transport of the 2017 Canadian wildfire plume to the tropics via the Asian monsoon circulation. *Atmospheric Chemistry and Physics*, *19*(21), 13547–13567. https://doi.org/10.5194/acp-19-13547-2019

Letertre-Danczak, J., Benedetti, A., Quesada-Ruiz, S., Dabas, A., & Flament, T. (2020). The ESA-funded Aeolus/EarthCare Aerosol Assimilation Study (A3S). In *EGU General Assembly 2020*, Online 4–8 May 2020, EGU2020-21436. https://doi.org/10.5194/egusphere-egu2020-21436

Lux, O., Lemmerz, C., Weiler, F., Marksteiner, U., Witschas, B., Rahm, S., et al. (2020). Intercomparison of wind observations from the European Space Agency's Aeolus satellite mission and the ALADIN Airborne Demonstrator. *Atmospheric Measurement Techniques*, *13*, 2075–2097. https://doi.org/10.5194/amt-13-2075-2020

Mamouri, R.-E., & Ansmann, A. (2016). Potential of polarization lidar to provide profiles of CCN- and INP-relevant aerosol parameters. *Atmospheric Chemistry and Physics*, *16*(9), 5905–5931. https://doi.org/10.5194/acp-16-5905-2016

Martin, A., Weissmann, M., Reitebuch, O., Rennie, M., Geiß, A., & Cress, A. (2021). Validation of Aeolus winds using radiosonde observations and numerical weather prediction model equivalents. *Atmospheric Measurement Techniques*, *14*(3), 2167–2183. https://doi.org/10.5194/amt-14-2167-2021

Ohneiser, K., Ansmann, A., Baars, H., Seifert, P., Barja, B., Jimenez, C., et al. (2020). Smoke of extreme Australian bushfires observed in the stratosphere over Punta Arenas, Chile, in January 2020: Optical thickness, lidar ratios, and depolarization ratios at 355 and 532 nm. *Atmospheric Chemistry and Physics*, *20*(13), 8003–8015. https://doi.org/10.5194/acp-20-8003-2020

Papagiannopoulos, N., Mona, L., Alados-Arboledas, L., Amiridis, V., Baars, H., Binietoglou, I., et al. (2016). CALIPSO climatological products: Evaluation and suggestions from EARLINET. *Atmospheric Chemistry and Physics*, *16*(4), 2341–2357. https://doi.org/10.5194/acp-16-2341-2016

Pappalardo, G., Amodeo, A., Apituley, A., Comeron, A., Freudenthaler, V., Linné, H., et al. (2014). EARLINET: Toward an advanced sustainable European aerosol lidar network. *Atmospheric Measurement Techniques*, *7*(8), 2389–2409. https://doi.org/10.5194/amt-7-2389-2014

Pappalardo, G., Mona, L., D'Amico, G., Wandinger, U., Adam, M., Amodeo, A., et al. (2013). Four-dimensional distribution of the 2010 Eyjafjallajökull volcanic cloud over Europe observed by EARLINET. *Atmospheric Chemistry and Physics*, *13*(8), 4429–4450. https://doi.org/10.5194/acp-13-4429-2013

Peterson, D. A., Campbell, J. R., Hyer, E. J., Fromm, M. D., Kablick, G. P., Cossuth, J. H., et al. (2018). Wildfire-driven thunderstorms cause a volcano-like stratospheric injection of smoke. *NPJ Climate and Atmospheric Science*, *1*. https://doi.org/10.1038/s41612-018-0039-3

Pisso, I., Sollum, E., Grythe, H., Kristiansen, N. I., Cassiani, M., Eckhardt, S., et al. (2019). The Lagrangian particle dispersion model FLEXPART version 10.4. *Geoscientific Model Development*, *12*(12), 4955–4997. https://doi.org/10.5194/gmd-12-4955-2019

Radenz, M., Seifert, P., Baars, H., Floutsi, A. A., Yin, Z., & Bühl, J. (2021). Automated time-height-resolved airmass source attribution for profiling remote sensing applications. *Atmospheric Chemistry and Physics*, *21*(4), 3015–3033. https://doi.org/10.5194/acp-21-3015-2021

Reitebuch, O. (2012). The Spaceborne Wind Lidar Mission ADM-Aeolus. In U. Schumann (Ed.), *Atmospheric physics: Background – methods – trends* (pp. 815–827). Springer. https://doi.org/10.1007/978-3-642-30183-4_49

Reitebuch, O., Lemmerz, C., Lux, O., Marksteiner, U., Rahm, S., Weiler, F., et al. (2020). Initial assessment of the performance of the first Wind Lidar in space on Aeolus. *EPJ Web of Conferences*, *237*, 01010. https://doi.org/10.1051/epjconf/202023701010

Rennie, M., & Isaksen, L. (2020). *The NWP impact of Aeolus level-2B winds at ECMWF. (864)*. Retrieved from https://doi.org/10.21957/alift7mhr

Santillan, D., Huber, D., Meringer, M., Reitebuch, O., Schindler, F., & Weiler, F. (2019). VirES for Aeolus - Online visual analysis of Aeolus data. In *ESA living planet symposium 2019, Milan, Italy*. Retrieved from https://elib.dlr.de/130561/

Stoffelen, A., Pailleux, J., Källén, E., Vaughan, J. M., Isaksen, L., Flamant, P., et al. (2005). The atmospheric dynamics mission for global wind field measurement. *Bulletin of the American Meteorological Society*, *86*(1), 73–88. https://doi.org/10.1175/BAMS-86-1-73

Stohl, A., Eckhardt, S., Forster, C., James, P., Spichtinger, N., & Seibert, P. (2002). A replacement for simple back trajectory calculations in the interpretation of atmospheric trace substance measurements. *Atmospheric Environment*, *36*(29), 4635–4648. https://doi.org/10.1016/s1352-2310(02)00416-8

Straume, A. G., Rennie, M., Isaksen, L., de Kloe, J., Marseille, G.-J., Stoffelen, A., et al. (2020). ESA's space-based doppler wind lidar mission Aeolus - First wind and aerosol product assessment results. *EPJ Web of Conferences*, *237*, 01007. https://doi.org/10.1051/epjconf/202023701007

Tesche, M., Wandinger, U., Ansmann, A., Althausen, D., Müller, D., & Omar, A. H. (2013). Ground-based validation of CALIPSO observations of dust and smoke in the Cape Verde region. *Journal of Geophysical Research: Atmospheres*, *118*(7), 2889–2902. Retrieved from https://doi.org/10.1002/jgrd.50248

Val Martin, M., Kahn, R. A., & Tosca, M. G. (2018). A global analysis of wildfire smoke injection heights derived from space-based multi-angle imaging. *Remote Sensing*, *10*(10). https://doi.org/10.3390/rs10101609

Wandinger, U. (1998). Multiple-scattering influence on extinction- and backscatter-coefficient measurements with Raman and high-spectral-resolution lidars. *Applied Optics*, *37*(3), 417–427. https://doi.org/10.1364/AO.37.000417

Wandinger, U., Baars, H., Engelmann, R., Hünerbein, A., Horn, S., Kanitz, T., et al. (2016). HETEAC: The aerosol classification model for EarthCARE. *EPJ Web of Conferences*, *119*, 01004. https://doi.org/10.1051/epjconf/201611901004

Wehner, M., Arnold, J., Knutson, T., Kunkel, K., & LeGrande, A. (2017). Droughts, Floods, and Wildfires. In D. J. Wuebbles, D. W. Fahey, K. A. Hibbard, D. J. Dokken, B. C. Stewart, & T. K. Maycock (Eds.), *Climate Science Special Report: Fourth National Climate Assessment*, Volume I (pp. 231–256). Washington, DC: U.S. Global Change Research Program. https://doi.org/10.7930/j0cj8bnn

Winker, D. M., Vaughan, M. A., Omar, A., Hu, Y., Powell, K. A., Liu, Z., et al. (2009). Overview of the CALIPSO mission and CALIOP data processing algorithms. *Journal of Atmospheric and Oceanic Technology*, *26*(11), 2310–2323. https://doi.org/10.1175/2009jtecha1281.1

Witschas, B., Lemmerz, C., Geiß, A., Lux, O., Marksteiner, U., Rahm, S., et al. (2020). First validation of Aeolus wind observations by airborne Doppler wind lidar measurements. *Atmospheric Measurement Techniques*, *13*(5), 2381–2396. https://doi.org/10.5194/amt-13-2381-2020

Young, S. A., Vaughan, M. A., Garnier, A., Tackett, J. L., Lambeth, J. D., & Powell, K. A. (2018). Extinction and optical depth retrievals for CALIPSO's Version 4 data release. *Atmospheric Measurement Techniques*, *11*(10), 5701–5727. https://doi.org/10.5194/amt-11-5701-2018